21st Australasian Fluid Mechanics Conference
Adelaide, Australia
10-13 December 2018

A Numerical Investigation of the Optimum Inclination Angle of Solar Chimney subject to Different Heat Fluxes

J. Kong, C. Lei and J. Niu

Centre for Wind, Waves and Water, School of Civil Engineering

The University of Sydney, Sydney, NSW 2006, Australia

Abstract

A numerical investigation has been conducted to identify optimum inclination angles of solar chimney under different heat fluxes and air gap widths. Steady-state CFD simulations are performed on a 2D standalone inclined roof-top solar chimney model with uniform heat fluxes ranging from 200W/m^2 to 800W/m^2. The absorber wall is 500-mm high and the air gap width varies from 20mm to 60mm. Inclination angles ranging from 30° to 90° relative to the horizontal plane are calculated. The results reveal that with the gradual increase of the inclination angle and the decrease of the air gap width, the mass flow rate through the solar chimney increases. For a vertical solar chimney with 20mm air gap width and 800W/m^2 heat flux, the mass flow rate is around 70% higher than that for a 60mm-gap and 30° inclined solar chimney under the same heat flux condition.

Introduction

Solar chimney, which is a thermo-syphoning channel to improve natural ventilation, has been extensively studied due to the worldwide energy crisis. It was reported that approximately 32 percent of the global energy consumption is related to buildings [12]. By creating an adequate temperature difference between the inside and outside of the solar chimney channel, the relatively hot air rises up and thus a buoyancy-driven ventilating flow can be induced. DeBlois, Bilec and Schaefer [4] reported that, because of the potential cooling load reduction provided by natural ventilation, almost 20 percent of the electrical energy was saved with natural ventilation strategies.

Common configurations of solar chimney can be classified into two categories: wall-attached solar chimney and roof-top solar chimney. One of the limitations of the vertical wall-attached solar chimney is its inability to receive maximum solar radiation due to the steep angle between the incoming sun light and the absorber wall. In addition, the presence of the absorber wall on the sun-facing side sacrifices the daylight coming into the building, and thus reduces the comfort level. Therefore, roof-top solar chimney which can be conveniently installed without altering the existing building structure, has received massive research attention. This study focuses on a window-sized rooftop-mounted solar chimney and aims to investigate the performance of such a small chimney. Further, the present study will identify the optimum inclination angle and air gap width under different solar irradiance.

Problem Formulation

Figure 1 depicts the schematic of the two-dimensional solar chimney model under consideration. The length of the solar chimney is fixed at 500mm. Three different air gap widths (20mm, 40mm and 60mm) and five different inclination angles (30°, 45°, 60°, 75° and 90° from the horizontal) are calculated. The absorber wall is heated by the uniform heat fluxes ranging from 200 W/m^2 to 800W/m^2. The Rayleigh number is the major parameter to characterize the convective heat transfer in the solar chimney, which is defined as follows:

$$Ra = \frac{g\beta q'' H_a^4}{\alpha \nu \kappa} \quad (1)$$

where Ra is the Rayleigh number, g is the gravitational acceleration (m/s^2), β is the thermal expansion coefficient (1/K), q'' is the input heat flux (W/m^2), Ha is the absorber height (m), α is the thermal diffusivity (m^2/s), ν is the kinematic viscosity (m^2/s) and κ is the thermal conductivity (W/m K).

According to Chen, et al. [3], the transition from laminar to turbulence in a solar chimney channel occurs when the Rayleigh number exceeds 2×10^{13}. Since the maximum Rayleigh number in the present solar chimney is only 1.8×10^{11}, the flow in the solar chimney channel is considered as laminar.

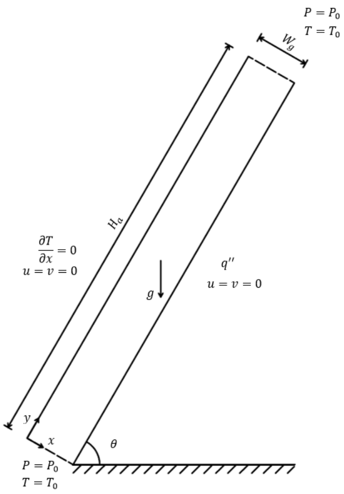

Figure 1. Schematic of solar chimney system with boundary conditions.

Since the temperature differences between the inside and outside of the solar chimney are not too large, i.e. $\beta(T-T_0) \ll 1$, Boussinesq approximation is adopted. The simplified two-dimensional steady-state equations governing the mass, momentum and energy conservation are written as follows:

$$\frac{\partial u}{\partial x} + \frac{\partial v}{\partial y} = 0 \quad (2)$$

$$u\frac{\partial u}{\partial x} + v\frac{\partial u}{\partial y} = -\frac{1}{\rho}\frac{\partial P}{\partial x} + \nu(\frac{\partial^2 u}{\partial x^2} + \frac{\partial^2 u}{\partial y^2}) + g\beta(T-T_0)\cos\theta \quad (3)$$

$$u\frac{\partial v}{\partial x} + v\frac{\partial v}{\partial y} = -\frac{1}{\rho}\frac{\partial P}{\partial y} + \nu\left(\frac{\partial^2 v}{\partial x^2} + \frac{\partial^2 v}{\partial y^2}\right) + g\beta(T-T_0)\,sin\,\theta \quad (4)$$

$$u\frac{\partial T}{\partial x} + v\frac{\partial T}{\partial y} = \alpha(\frac{\partial^2 T}{\partial x^2} + \frac{\partial^2 T}{\partial y^2}) \quad (5)$$

Numerical Methods

The computational domain consists of inlet, outlet, glazing and absorber wall. The operating temperature is set to 300K.

Pressure inlet and pressure outlet conditions are prescribed at the bottom and top apertures of the channel respectively. The inlet and outlet pressure is the same as the ambient pressure, and any flow entering the channel is at the ambient temperature. A stationary no-slip wall condition is applied to both the glazing and absorber wall. Moreover, a constant uniform heat flux q'' is applied to the absorber wall and the glazing is assumed to be adiabatic. The change of the inclination angle is implemented through altering the direction of the gravitational acceleration.

A finite volume solver is adopted to solve the above equations. The SIMPLE scheme is used to couple the pressure and the velocity. In terms of spatial discretization, the PRESTO! scheme is adopted for pressure and the second order upwind scheme is adopted for both momentum and energy equations.

The computational domain is divided into three regions for mesh construction with non-uniform quadrilateral meshes near the boundaries and uniform meshes in the middle region. The growth rate of the mesh size in the direction normal to the surfaces is 1.05. In order to ensure that there are at least 7 layers of meshes in the thermal boundary layer, the scale $\delta_{Ts} \sim \frac{H_a}{(RaPr)^{1/5}}$ is used to estimate the steady-state thermal boundary layer thickness [8]. The accuracy of the numerical results are determined by mesh sensitivity test and residual test. Three meshes of 66×500, 132×1000 and 264×2000 and three residuals of 10^{-4}, 10^{-6} and 10^{-8} are tested under the highest heat flux, i.e. 800W/m^2. It is found that the 66×500 mesh with 10^{-4} residual is adequate to resolve the problem with less than 0.5% deviation of the predicted mass flow rate compared to that obtained with the finest mesh.

Results and Discussion

Inclination Angle Effect

Prasad and Chandra [10] reported that the vertical solar chimney offers the maximum air flow rate when the absorber wall is subject to a given amount of insolation. This is mainly because for a given chimney channel, the fully upright configuration results in the highest stack height than tilted configurations. Thus the vertical solar chimney is preferred for the greatest buoyancy effects. Thong, Quaan and Seng [11] did numerical simulations on a 2-m long solar roof collector with inclination angles varying from 15° to 55° relative to the horizontal plane and also demonstrated that the higher the inclination angle, the stronger the induced natural ventilation.

Figure 2 depicts the calculated outlet mass flow rate of a solar chimney with a 0.04-m air gap width under different inclination angles and heat fluxes. It can be seen that the mass flow rate peaks at 90° regardless of the heat flux. Moreover, a higher heat flux causes an increased mass flow rate due to higher buoyancy effects inside the solar chimney. It is interesting to note that, although the four calculated heat fluxes are equally spaced, the increment of the mass flow rate due to the increasing heat flux decreases as the heat flux gets higher. This is because as heat flux increases, the buoyancy effect is enhanced and the thermal boundary layer becomes thinner. As a result, a reverse flow is more likely to occur at the exit of the chimney channel. Consequently the increment of the mass flow rate reduces. The same tendency is also observed for solar chimneys with 0.02-m and 0.06-m air gap widths, respectively.

In order to understand the correlations between the predicted mass flow rate and the inclination angle, profiles of the outlet *y* velocity of a solar chimney with different inclination angles are plotted in Figure 3. It can be seen that near the absorber wall, the *y* velocity increases with the increasing inclination angle. It could be explained by the fact that, the *y* velocity in the thermal boundary layer increases with the inclination angle due to the increase of buoyancy effects. This result is similar to the experimental observation of Chen et al. [3]. On the other hand, negative *y* velocities can be observed near the glazing, which suggests reverse flow occurs there. Although it can be seen that, when the inclination angle increases, stronger reverse flow is present, the overall mass flow rate still increases with the inclination angle. However, the experimental data of Chen et al. [3] and Zhai, Dai and Wang [13] showed that the 45° inclined solar chimney offered the maximum air flow rate. They argued that this was because the pressure loss was higher and the heat transfer coefficient was lower for the vertical solar chimney although it has the highest stack height. A possible reason for the discrepancy between the previous experiment and the present numerical simulation may be because the boundary layer was not properly resolved during the previous velocity measurement. As we can see in figure 3, the relatively high velocity is present over a short distance from the absorber wall. If this region is not properly resolved, it may significantly affect the accuracy of the measured flow rate.

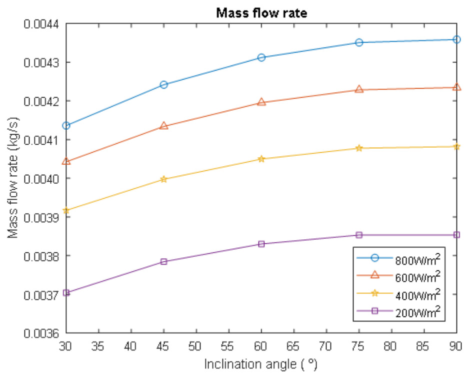

Figure 2. Outlet mass flow rates for a chimney with a 0.5-m height and a 0.04-m air gap width at the inclination angles of 30° to 90° subject to input heat fluxes from 200W/m^2 to 800W/m^2.

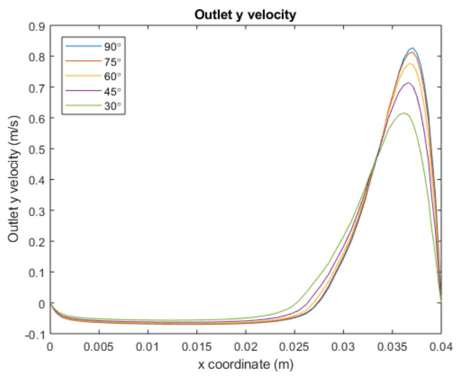

Figure 3. Outlet *y* velocity for a solar chimney of 0.5-m height and 0.04-m air gap width under 800 W/m^2 heat flux.

As is mentioned above, reverse flow can be detected at the chimney outlet. In order to obtain a better understanding of the effect of the reverse flow on the flow behaviour in the solar chimney, contours of stream functions of a vertical and an inclined solar chimney under the highest heat flux conditions are plotted in Figure 4. It is clear that the flow domain is split into two distinctive regions: buoyancy-driven flow region and reverse flow region. In order to quantify the penetration of reverse flow into the chimney channel, penetration depth and width are visualized and defined in Figure 5, with the blue area representing buoyancy-driven flow region and the red area representing the reverse flow region, regardless of inclination angle and air gap width. It is seen in figure 4 that, with the reduced inclination angle, the reverse flow is slightly reduced. For a solar chimney with a height of 0.5m and an air gap width of 0.04m subject to an input heat flux of 800 W/m^2, the penetration depth and width obtained with an inclination angle of 45° is approximately 5% less than that with the upright configuration. This phenomenon can be explained by the inverse relationship between the thermal boundary layer thickness and the reverse flow. As can be seen in Table 1, solar chimney with a smaller inclination angles has a thicker thermal boundary layer, leaving less room for the reverse flow to develop. Therefore, as the inclination angle decreases, the reverse flow tends to be suppressed, with its penetration depth and width reduced.

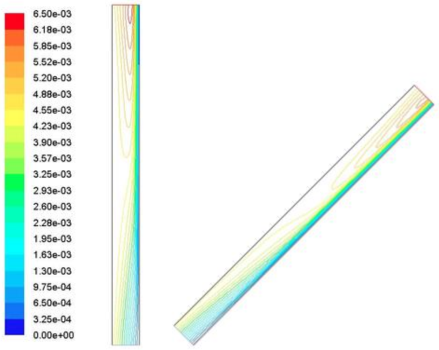

Figure 4. Stream functions (from 0 kg/s to 6.50×10^{-3} kg/s with an interval of 3.25×10^{-4} kg/s) for a solar chimney of 0.5-m height and 0.04-m air gap width at the inclination angles of 90° (left) and 45° (right) under 800 W/m^2 heat flux.

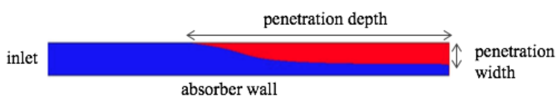

Figure 5. Representation of distinctive flow regions in a solar chimney channel, regardless of inclination angle and air gap width (blue area: buoyancy-driven flow region, red area: reverse flow region).

Outlet thermal boundary layer thickness (m)					
Heat flux (W/m^2)	Inclination Angle (°)				
	30	45	60	75	90
800	0.0153	0.0142	0.0135	0.0130	0.0128
600	0.0165	0.0150	0.0142	0.0137	0.0136
400	0.0180	0.0160	0.0152	0.0150	0.0149
200	0.0205	0.0188	0.0175	0.0173	0.0167

Table 1. Outlet thermal boundary layer thickness for a solar chimney of 0.5-m height and 0.04-m air gap width.

Gan [5] noted that the size of the computational domain may affect the predicted performance of the solar chimney, especially through affecting the reverse flow. In order to eliminate the effect of the domain size, we also carried out simulations in a very large computational domain that fully encompasses the current air channel. The results show that the reverse flow is reduced and the predicted mass flow rate increases with the larger computational domain for all the calculated inclination angles and heat fluxes. However, the vertical solar chimney still performs the best. This is probably due to the fact that, compared with the increase in the boundary layer velocity, the slight increase of reverse flow caused by the increase of inclination angle has little impact on the overall mass flow rate, as suggested in Figure 3. Other parameters such as the stack height may play a more significant role than the penetration depth (width) of the reverse flow in determining the mass flow rate.

Figure 6 shows the outlet average temperature of the solar chimney. It can be seen that the overall trend is that the average temperature increases with decreasing inclination angle for a given heat flux. This is because the residence time of the air is longer for inclined solar chimney. According to Chen et al. [3] and Andersen [1], the energy equation could be reduced to the following form because the terms for kinetic energy, potential energy and pressure work are much less than that of the internal energy term.

$$\dot{m}C_p\Delta T = q''H_aW_w \tag{6}$$

where C_p is the specific heat, ΔT is the temperature difference between the average temperature inside the channel and the ambient temperature, and W_w is the width of the solar chimney. The equation demonstrates that for a given heat flux, the reduced mass flow rate tends to cause larger temperature difference.

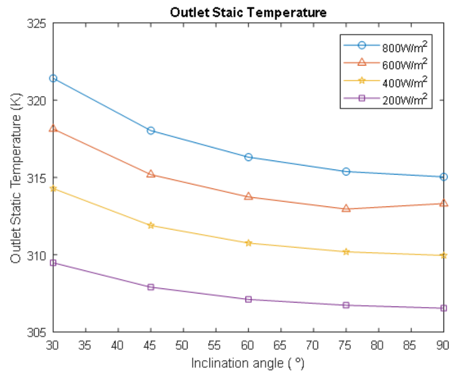

Figure 6. Outlet average static temperature for a solar chimney of 0.5-m height and 0.04-m air gap width.

Air Gap Width Effect

To investigate the possibility of improving the ventilation rate and reducing the friction experienced by the flow, simulations have been conducted to study the effects of the air gap width. Figure 7 presents the calculated outlet mass flow rates under different air gap widths and heat fluxes. It is found that the mass flow rate increases with the reduced air gap width, especially under higher heat fluxes. For the 800 W/m^2 input heat flux, the mass flow rate of a solar chimney of 0.02-m air gap width is approximately 60% higher than that of a solar chimney of 0.06-m air gap width under identical heat flux and inclination conditions. However, for the 200 W/m^2 input heat flux, the difference between the mass flow rates of the different air gap widths is reduced to 50%.

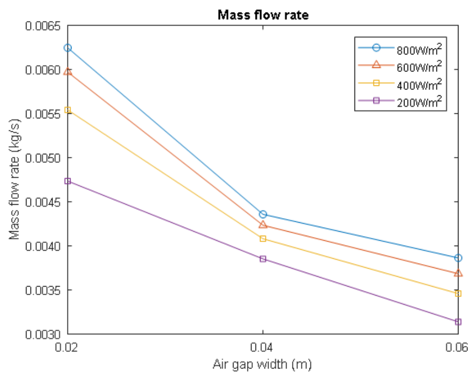

Figure 7. Outlet mass flow rate for a solar chimney of 0.5-m height and 90° inclination angle.

Figure 8 shows the contours of stream functions of the vertical solar chimney with 0.02-m, 0.04-m and 0.06-m air gap width, respectively. As can be seen in the figure, the reduction of the air gap width has a significant impact on the reverse flow. The same phenomenon is also observed in solar chimneys with other inclination angles. This is mainly because the narrow air gap width is closer to the thickness of the thermal boundary layer. Khanal and Lei [7] studied an inclined passive wall solar chimney and revealed that the maximum mass flow rate could be achieved when the outlet air gap width was the same as the steady-state thermal boundary layer thickness. In addition, the experimental investigation conducted by the same authors confirmed the claim [9].

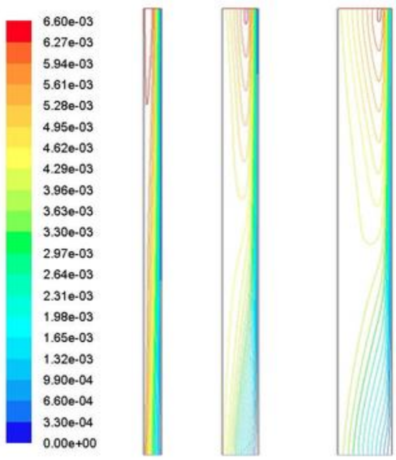

Figure 8. Stream functions (from 0 kg/s to 6.60×10^{-3} kg/s with an interval of 3.3×10^{-4} kg/s) for a solar chimney of 0.5-m height, 90° inclination angle under 0.02-m, 0.04-m and 0.06-m air gap width (left to right), respectively.

Some research reported in the literature showed the opposite results in that solar chimney with wider air gaps performed better [2, 6]. This may be because for the large air gap width the effects of pressure losses was less than the wall friction losses. However, many other factors such as the stack height, the surface roughness and so on may also contribute to the variations of the reported results. Therefore, care must be taken when making comparisons of or applying the results reported from different investigations. It is interesting to note that deduced from the trend shown in figure 7, the solar chimney with the 0.02m air gap width may not perform well for lower heat fluxes (below 200 W/m^2) as the thermal boundary layer is thicker and the flow resistance near the inlet and outlet is higher, and thus the pressure losses are expected to be higher.

Conclusions

In this study, a numerical simulation has been conducted to investigate the influence of the inclination angle and air gap width on the performance of solar chimney under different heat fluxes. Two main conclusions can be drawn from the study of a window-sized solar chimney:

1. Higher inclination angle relative to the horizontal plane gives better ventilation performance of the solar chimney due to the fact that the stack height is the dominant parameter.

2. For a solar chimney with a height of 0.5m and different inclination angles, the maximum mass flow rate is achieved with a 0.02-m air gap width due to the fact that this air gap width is closest to the thermal boundary layer thickness. However, wider solar chimney may perform better when the input heat flux is less than 200 W/m^2, with which the thermal boundary layer is thick enough to prevent the reverse flow.

It should be noted that in this paper solar radiation captured by the absorber wall is assumed to be the same for all inclination angles. In reality, the inclination angle change would also mean different incident solar intensity. It would be interesting to examine if there would exist an optimum inclination angle at any given solar altitude angle.

References

[1] Andersen, K.T., Theory for natural ventilation by thermal buoyancy in one zone with uniform temperature. *Building and Environment*, 2003. 38(11), pp.1281-1289.

[2] Burek, S.A.M. and A. Habeb, Air flow and thermal efficiency characteristics in solar chimneys and Trombe Walls. *Energy and Buildings*, 2007. 39(2): p. 128-135.

[3] Chen, Z.D., et al., An experimental investigation of a solar chimney model with uniform wall heat flux. *Building and Environment*, 2003. 38(7): p. 893-906.

[4] DeBlois, J., M. Bilec, and L. Schaefer, Simulating home cooling load reductions for a novel opaque roof solar chimney configuration. *Applied Energy*, 2013. 112: p. 142-151.

[5] Gan, G., Impact of computational domain on the prediction of buoyancy-driven ventilation cooling. *Building and Environment*, 2010. 45(5): p. 1173-1183.

[6] Hirunlabh, J., et al., Study of natural ventilation of houses by a metallic solar wall under tropical climate. *Renewable Energy*, 1999. 18(1): p. 109-119.

[7] Khanal, R. and C. Lei, Flow reversal effects on buoyancy induced air flow in a solar chimney. Solar Energy, 2012. 86(9): p. 2783-2794.

[8] Khanal, R. and C. Lei, A scaling investigation of the laminar convective flow in a solar chimney for natural ventilation. *International Journal of Heat and Fluid Flow*, 2014. 45(1): p. 98-108.

[9] Khanal, R. and C. Lei, An experimental investigation of an inclined passive wall solar chimney for natural ventilation. *Solar Energy*, 2014. 107: p. 461-474.

[10] Prasad, M. and K. Chandra, Optimum tilt of solar collector for maximum natural flow. *Energy Conversion and Management*, 1990. 30(4): p. 369-379.

[11] Thong, T.B., L.M. Quaan, and O.K. Seng. Simulations of flow in a solar roof collector driven by natural convection. in 16th Australasian Fluid Mechanics Conference, 16AFMC, December 3, 2007 - December 7, 2007. 2007. Gold Coast, QLD, Australia: University of Queensland.

[12] Ürge-Vorsatz, D., et al., Heating and cooling energy trends and drivers in buildings. *Renewable and Sustainable Energy Reviews*, 2015. 41: p. 85-98.

[13] Zhai, X., Y. Dai, and R. Wang, Experimental investigation on air heating and natural ventilation of a solar air collector. *Energy and Buildings*, 2005. 37(4): p. 373-38